Oxidation of a Molecule by the Biexcitonic State of a CdS Quantum Dot

*Shichen Lian[1,2], Joseph A. Christensen[1,2], Mohamad S. Kodaimati[1], Cameron R. Rogers[1], Michael R. Wasielewski[1,2], and Emily A. Weiss[1,2]**

[1]Department of Chemistry and [2]Center for Light Energy Activated Redox Processes (LEAP), Northwestern University, 2145 Sheridan Rd., Evanston, IL 60208-3113

*corresponding author. Email: e-weiss@northwestern.edu

ABSTRACT

This paper describes spectroscopic evidence for the photoinduced transfer of a hole from the biexcitonic state of a CdS quantum dot (QD) to a phenothiazine (PTZ) molecular acceptor, covalently linked to the QD through phenyldithiocarbamate (PTC), with power-dependent yields of 8% - 21%. Visible and near-infrared transient absorption spectroscopy (TA) data suggest that the mechanisms of hole extraction include direct hole transfer from the QD's valence band to PTZ in 2.4±0.2 ps, or trapping of holes at the QD surface in ~1 ps, followed by sequential hole transfer to PTZ. Both of these mechanisms potentially out-compete Auger recombination of biexcitonic states, which occurs within these QDs in 20±1 ps. These results suggest that the PTC linkage will be useful for extracting multiple holes from a QD photosensitizer or solo photocatalyst to drive multi-step oxidation reactions.

INTRODUCTION

Colloidal quantum dots (QDs) have emerged as promising photocatalysts and photosensitizers for organic synthesis[1-4] and production of fuels[5-10]. Most of these reports target multi-electron redox reactions such as reduction of protons[10-11] and carbon dioxide[12-14], water oxidation[15], and carbon-carbon coupling[1-3]. Such reactions depend on fast delivery of two or more electrons or holes from a photoexcited QD to a catalyst or directly to a substrate, so that the yield of the reaction does not depend on the lifetimes of one-electron intermediates. The conduction and valence bands of QDs have degenerate band-edge energy levels and can therefore accommodate multiple excitons simultaneously (*e.g.*, two band-edge excitons for CdSe and CdS, and four band-edge excitons for PbS and PbSe).[16-19] Biexcitons or higher-order excitons can form through photoexcitation under high fluence, or, if only a low-fluence source is available (like sunlight), through absorption of a single high-energy photon followed by a carrier multiplication process that creates two lower-energy excitons from a single high energy exciton.[20-22]

Creation of biexcitons in QDs is only useful for photocatalysis, however, if two of the relevant carrier (electrons or holes) can be extracted – that is, at a minimum, if the first electron or hole can be extracted before the biexciton decays to a single exciton *via* Auger recombination. For unshelled cadmium and lead chalcogenide QD cores, time constants for Auger recombination range from 10s to 100s of ps.[23-26] Coating the QD cores with additional semiconductor layers (such as CdSe, CdS, and ZnS) that create a type-II or quasi-type II core/shell heterojunction can decrease the Coulombic interaction between electrons and holes and slow the Auger process to nanoseconds.[27-31] The shelling approach however usually results in confinement of one of the charge carriers in the QD core, which dramatically lowers the turnover number of the QD catalyst. It is therefore important to design a system where both electrons and holes are extractable from the core, and, specifically, where the first catalytically relevant carrier is extractable from the biexcitonic state on a timescale competitive with Auger recombination.

Electron transfer from cadmium chalcogenide QDs to molecular acceptors is typically very fast (single picoseconds)[32-34]; several groups have demonstrated the extraction of photoinduced electrons from the biexcitonic states of unshelled QDs, either to multiple surface-adsorbed molecular acceptors[35] or a single electron acceptor that can accommodate two electrons[16]. Hole transfer from a QD to a molecule is usually much slower than Auger recombination (nanoseconds *vs.* 10-100 ps)[28, 36-38] due to the larger effective mass of the hole[39]. Parkinson and coworkers, in

2010, demonstrated two-electron extraction from biexcitons created by carrier multiplication, within PbS QDs to a TiO_2 film, followed by two-hole collection by the sulfide/polysulfide redox couple.[40] There exist no other reports of hole extraction from the biexcitonic (or even two-hole oxidized) state of a colloidal QD to a molecular acceptor.

Here, we demonstrate photoinduced hole extraction from the biexcitonic state of an unshelled CdS QD to a molecular acceptor, phenothiazine (PTZ), linked to the QD through a phenyldithiocarbamate (PTC) bridge. We[41-44] and others[45-50] have previously shown that the orbitals (particularly, the HOMO) of PTC mix with states of the QD valence band to produce interfacial states that delocalize the excitonic hole beyond its typical Bohr radius, resulting in enhanced electronic coupling between the excitonic hole and any molecule that is sufficiently coupled to PTC. We have also shown that, for certain binding geometries of PTC on the QD surface, the dithiocarbamate group can act as a hole trapping ligand rather than a hole delocalizing ligand.[42, 46]Although in past work we substituted the PTC linker with PTZ at the *para* position of PTC, here we attach it at the *meta* position, since we envision this compound to be a model compound for a doubly substituted (2-hole) acceptor. We find that a fraction of photo-oxidation of PTZ by the QD occurs through direct hole transfer from the QD core with a time constant that is ~10× faster than that of Auger recombination, and that PTZ can also be oxidized by holes that initially trap on the QD surface (in ~ 1ps) and then transfer to PTZ. Importantly, comparison of the yields of Auger recombination at various excitation pump energies for QDs with and without attached PTZ to the yields of $PTZ^{+\bullet}$ formed at these pump energies reveals that PTZ is oxidized by the biexcitonic states of the QDs with yields of 8% - 21%.

METHODS

Ground State and Time-Resolved Absorption Spectroscopy. Ground state absorption spectra of QD samples were obtained on a Varian Cary 5000 spectrometer in a 2 mm quartz cuvette in THF-*d8*. All spectra were baseline-corrected with a THF-*d8* sample. Our transient absorption spectroscopy setup is described elsewhere.[51] TA samples were prepared in 2 mm quartz cuvettes in a N_2 glovebox and were measured under constant stirring. The THF-*d8* used in both ground-state and time-resolved experiments was degassed through three freeze-pump-thaw cycles.

Nuclear Magnetic Resonance Spectroscopy. All ^1H NMR spectra of QD samples were acquired in THF-*d8* on an Agilent DD2 600 MHz spectrometer (128 scans with a relaxation delay

time of 2 s). ^{1}H NMR spectra of functionalized PTZ molecules were acquired on a Bruker Avance III 500 MHz spectrometer (32 scans with a relaxation delay time of 1 s).

RESULTS AND DISCUSSION

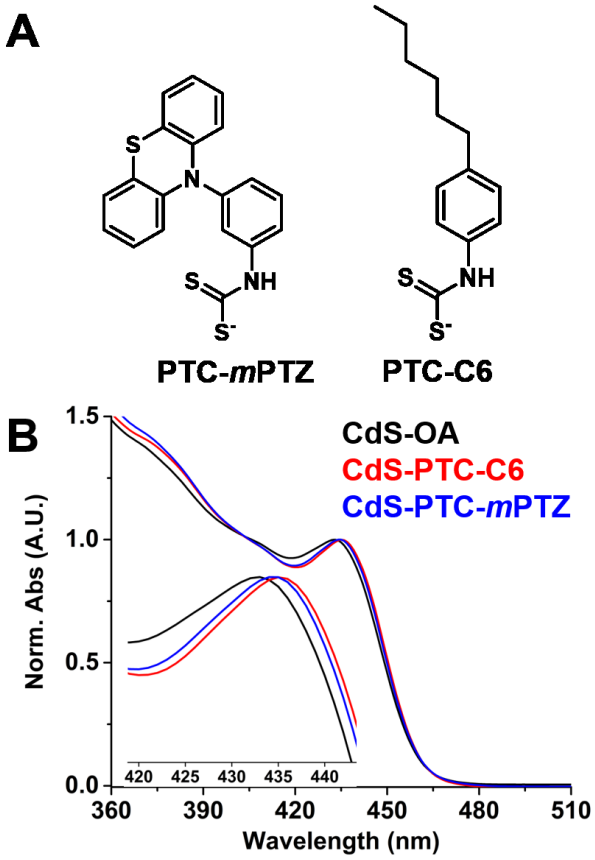

Figure 1. (A) Anionic forms of functionalized PTC ligands used in this study. **(B)** Normalized ground-state absorption spectra of CdS QDs in THF-d_8 capped with native oleate ligands (black), with 20±5 eq. of bound PTC-C6 (red line) and 20±5 eq. of bound PTC- *m*PTZ (blue), measured by solution ^{1}H NMR. **Inset**: zoomed-in region of the lowest-energy absorption peaks of the three samples.

Preparation of Oleate-capped QDs and Synthesis of PTC Ligands. Oleate-capped CdS QDs are synthesized using a literature procedure.[52] As-synthesized QDs are stored in hexanes at room temperature in the dark. PTC-C6 (**Figure 1A**) is synthesized using a literature procedure[52], and as-synthesized PTC-C6 is stored in a freezer to prevent thermal degradation. The PTC-*m*PTZ molecule (**Figure 1A**) is synthesized based on the literature procedure for the *para*-substituted PTC-PTZ molecule[39] and stored in a freezer (see the SI for details and ^{1}H NMR spectra).

Preparation of CdS-PTC-R (R = C6 or *m*PTZ) Complexes. The PTC-functionalized QDs were prepared by adding 30 equivalents of PTC-C6 or PTC-*m*PTZ triethylammonium salts into a sample of oleate-capped CdS QDs, dispersed in air-free THF-*d8*, inside a nitrogen glovebox. We use PTC-C6-capped QDs, rather than oleate-capped QDs, as control systems for our experiments, because it has been shown that the PTC headgroup influences the photophysical properties of QDs.[45, 48] Addition of a redox-inert hexyl tail to PTC increases the solubility of PTC-capped QDs in THF significantly, relative to PTC alone, and facilitates optical and NMR measurements.

We used a well-established ^{1}H NMR procedure to quantify the surface coverage of both types of PTC ligands on the QD (see Figure S1 in the SI). We have demonstrated previously that one dithiocarbamate binding group displaces, on average, two bound oleate species from the cation-enriched surface of CdS QDs, in the form of $Cd(oleate)_2$,[39, 52] where the net charge at the surface of the particle is balanced by PTC's triethylammonium counterion, as evidenced by the broadening of its NMR signals upon adsorption.[52] We therefore quantify the number of bound PTC-C6 or PTC-*m*PTZ ligands per QD by counting the number of displaced bound oleate on the surface of QDs (~40±10) and inferring that both PTC-C6 and PTC- *m*PTZ samples have 20±5 bound PTC ligands per QD (with the remainder of the surface coated by oleate). The error bars are standard deviations calculated from NMR measurements on three separately prepared samples of each type of QD.

The CdS QDs used in this system have a first excitonic absorption peak at 430 nm, which corresponds to QD cores with an average radius of 2.3 nm.[53] The excitonic peaks are shifted to lower energy by 5 nm within the spectrum of the PTC-C6-coated QDs, and by 4 nm within the spectrum of the PTC-*m*PTZ-coated QDs, from those of oleate-capped QDs (**Figure 1B**), as expected from treatment of CdS QDs of this size with a low concentration of PTC-X ligand.[52]

Dynamics of Auger Recombination. We quantify the rate of Auger recombination of biexcitons created within the QD core by fitting kinetic traces extracted from the ground state bleach (GSB) feature (peaked at ~435 nm) within the TA spectra of the PTC-C6-capped QDs, pumped at 420 nm at a series of excitation powers (100 µW to 1000 µW) corresponding to pump energies between 0.2 µJ and 2 µJ. We only consider creation of biexcitons (as opposed to higher-order excitons) because the degeneracy of the lowest excitonic state ($1S_e$-$1S_{3/2}$) of a spherical CdS QD is 2-fold, and our 420-nm (100 meV above band-edge) excitation energy is not enough to access the next allowed transition ($1P_e$-$1P_{3/2}$) for CdS QDs of this

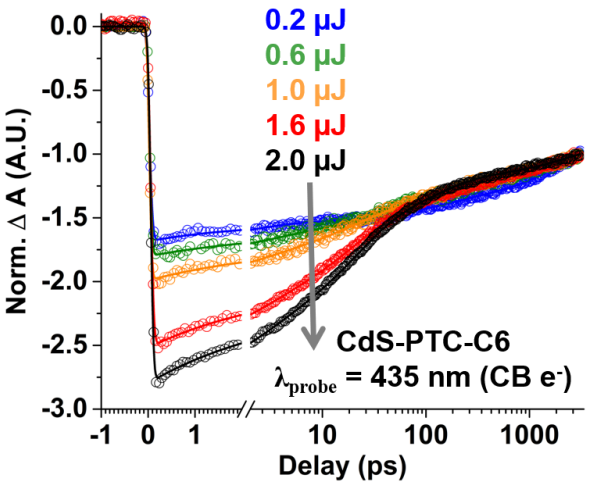

Figure 2. Normalized kinetic traces extracted from a representative set of TA measurements on CdS-PTC-C6 QDs in THF-d_8, photoexcited at 420 nm with increasing pump energies labelled in the legend, probed at 435 nm (the peak of the QD ground state bleach feature).

size.[54-57] The dynamics of the GSB only reflect the dynamics of conduction band-edge electrons in CdS QDs.[32] Fitting the kinetic trace for the GSB of the CdS-PTC-C6 samples collected under low photon fluence (0.2 μJ, corresponding to an expectation value of excitons, $\langle N \rangle$ of 0.24 per QD, see Figure S2 in the SI for details) yields four time constants: 2.1±0.2 ps, 110±10 ps, 2600±300 ps, and >3 ns (beyond our time window) (**Figure 2**). We assign the shortest two time constants to electron trapping processes, based on literature assignments.[32, 58-60] Considering the low quantum yield of QDs capped with PTC (<1%)[42], the two longer components likely correspond to non-radiative recombination of conduction band-edge electrons with trapped holes (discussed below).

When fitting the GSB kinetic traces at λ_{probe} = 435 nm after pumping with higher pump energies (0.6 μJ – 2 μJ), we fix the values of the four time constants extracted from the fit of the dynamics at 0.2 μJ pump energy (allowing their amplitudes to float), and add one additional component to account for the Auger recombination process, see Table S2 and fits in **Figure 2**. This process yields time constants for Auger recombination of between 20±1 ps (at 0.6 μJ) and 16±2 ps (at 2 μJ), which are consistent with previous reports for CdS QDs of this size.[23] Extraction of a hole from the biexcitonic state in these QDs would therefore require a first hole transfer that is competitive with a ~20-ps Auger process.

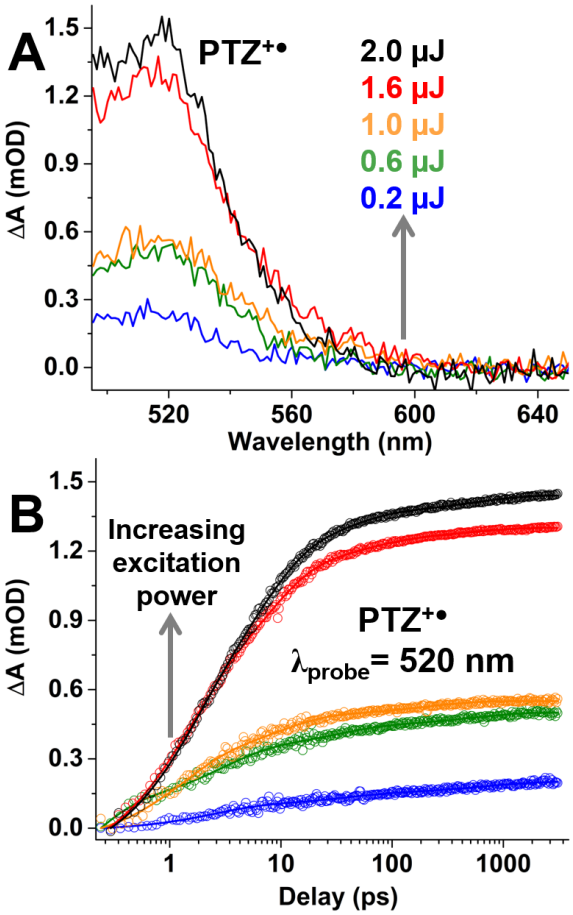

Figure 3. (A) Representative TA spectra of CdS-PTC-*m*PTZ at 3 ns, after subtracting the contribution from the photoinduced absorption (PIA) of QDs, collected with pump energies labeled in the legend. **(B)** Kinetic trace of the formation of $PTZ^{+\bullet}$, obtained from the deconvolution procedure described in the text.

Evidence for Photo-oxidation of PTZ in the CdS-PTC-*m*PTZ Complex. Hole transfer from the QD to the PTZ acceptor is confirmed by the appearance of the characteristic absorption peak of $PTZ^{+\bullet}$ in the TA spectra at 520 nm.[61] This absorption overlaps with the broad excited state absorptions of the QD (referred to as the "QD shelf") between ~480 nm and ~700 nm.[62] We obtained a pure spectrum of the QD shelf from the TA data of CdS-PTC-C6 samples with the same ligand surface coverages and excitation densities as those we used for CdS-PTC-*m*PTZ. We then obtained a pure spectrum of $PTZ^{+\bullet}$ by (i) scaling this pure shelf spectrum so that it matches the raw TA spectrum of CdS-PTC-*m*PTZ between 600 nm to 700 nm, a region where $PTZ^{+\bullet}$ does not absorb, and (ii) subtracting the pure shelf spectrum from the raw spectrum of CdS-PTC-*m*PTZ sample at a late time point (~3 ns) when the hole transfer process is complete. **Figure 3A** shows the pure $PTZ^{+\bullet}$ spectrum, and confirms the photo-oxidation of PTZ by the QDs.

Dynamics of Hole Trapping and Hole Extraction. With the pure $PTZ^{+\bullet}$ and QD excited state ("shelf") spectra, obtained as described directly above, as basis spectra, we used a previously reported algorithm to deconvolve the raw TA data for the CdS-PTC-*m*PTZ samples at all time-points into a linear combination of the two features.[39, 63] The similarity between the kinetic trace for the QD shelf feature obtained with the deconvolution procedure and the kinetic trace extracted from the raw (convolved) TA spectrum at 670 nm, where $PTZ^{+\bullet}$ does not absorb, confirms the accuracy of this deconvolution, see Figure S3 in the SI.

Figure 3B shows a representative set of deconvolved kinetic traces corresponding exclusively to the formation of $PTZ^{+\bullet}$ after pumping CdS-PTC-*m*PTZ at a series of different excitation densities. All traces can be fit adequately with a sum of three simple exponential terms. Under 0.2 μJ pump energies, the corresponding time constants are τ_{hT1} = 2.4±0.2 ps, τ_{hT2} = 35±5 ps, τ_{hT3} = 700±100 ps (**Table 1**; Table S3 contains data for higher pump energies). Each of these time constants must correspond to a photo-induced hole transfer process (hence their abbreviations τ_{hT1}, etc.) because photoinduced hole transfer from the QD to PTZ is the only means of producing $PTZ^{+\bullet}$ in this system.[34, 39, 61, 64]

To identify the mechanisms of hole transfer corresponding to the time constants for $PTZ^{+\bullet}$ formation listed in **Table 1**, we first determine the fate of photoinduced holes in the QDs without PTZ present. **Figure 4A** shows a set of raw TA kinetic traces extracted at 670 nm for CdS-PTC-C6. This probe wavelength is within the broad set of photoinduced absorptions of the aforementioned "QD shelf", primarily comprising contributions from absorptions of conduction band electrons and trapped holes on the QD core and in surface states.[62, 64] Consistent with previous reports[39, 62, 64], the dynamics for the CdS-PTC-C6 samples in this region (500 nm - 680 nm) are wavelength-independent (Figure S4). Most of the signal and dynamics at 670 can be accounted for by conduction band electrons, as evidenced by the large instrument limited rise at 670 nm, and similarity of decays of the kinetic traces at 670 nm and at the GSB (compare light blue traces in **Figure 4B**). Unlike the GSB, however, the kinetic trace at 670 nm for the CdS-PTC-C6 sample (collected at 100 μW) has an initial fast, but measurable, rise: τ_{rise1} = 1.1±0.1 ps, **Table 1.** This time constant matches a fast decay (τ_{decay1} = 1.3±0.1 ps in **Table 1**) at 1400 nm (primarily valence band holes)[51, 65] of the same sample, and therefore can be assigned to hole trapping from the valence band to a lattice or surface trap. This hole trapping process increases in rate with increasing excitation pump energy – τ_{rise1} = 0.8±0.1 ps at 2 μJ, see **Figure 4A** and Table S4 – probably due to increased density of valence band holes.

Although difficult to discern from inspection of **Figure 4B**, fitting of the kinetic traces in this figure shows that, upon introduction of PTZ, the absolute population of trapped holes decreases, evidenced by decreases in A_{rise1}, the amplitude of the hole trapping component in the kinetic trace at 670 nm, and A_{decay1}, the % of the total amplitude of decay at 1400 nm attributed to hole trapping (**Table 1**). This decrease in the *yield* of hole trapping upon introduction of PTZ occurs in spite of

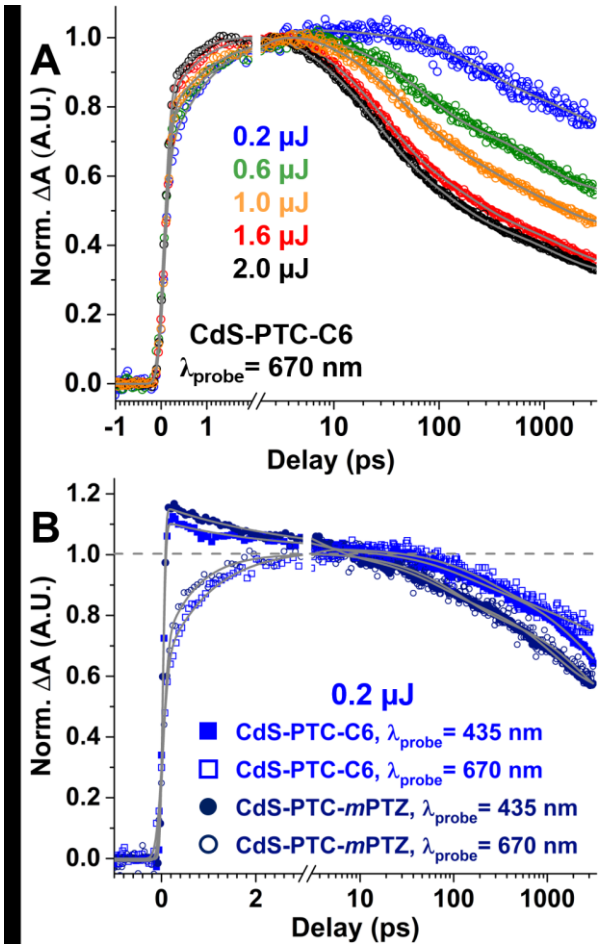

Figure 4. Normalized kinetic traces extracted from a representative set of TA measurements on CdS-PTC-C6 QDs in THF-d_8, photoexcited at 420 nm with increasing excitation pump energy labelled in the legend, probed 670 nm (the QD shelf). **(B)** Normalized Kinetic traces extracted at 670 nm (open squares and circles) and 435 nm (solid squares and circles) of the TA data from CdS-PTC-C6 (light blue) and CdS-PTC-*m*PTZ (navy blue), collected with 0.2 μJ excitation.

a slight increase in the apparent *rate* of hole trapping (from 1.1±0.1 ps without PTZ to 0.8±0.1 ps with PTZ), **Figure 4B** and **Table 1**. The latter is probably due to a convolution of hole trapping and direct hole transfer to PTZ in our observed time constant.[66-67] We suspect the decrease in yield of hole trapping is due to direct hole transfer from the VB of the QDs to PTZ, discussed below.

Differences between samples with and without PTZ are also apparent in the lifetimes of these trapped holes. **Table 1** also lists the amplitude-averaged lifetimes of the signal at 670 nm; for 0.2 μJ excitation, τ_{ave} at 670 nm decreases from 1400±400 ps to 690±60 ps upon introduction of PTZ. Most of this change can be accounted for by acceleration of decay of CB electrons upon introduction of PTZ (compare light blue and navy blue solid traces in **Figure 4B)**. There is, however, a long-lived population of trapped holes[61-62, 64] in CdS-PTC-C6 that creates a mis-match of the kinetic traces of the GSB and 670-nm at t > 1 ns (compare light blue traces in **Figure 4B**). This population disappears upon introduction of PTZ (compare navy blue traces in **Figure 4B**). We therefore suspect that PTZ can be oxidized by trapped holes. This result is significant because the hole trapping process is fast enough (~1 ps) to compete with Auger recombination of a biexciton (~20 ps), and therefore provides an additional pathway for oxidation of PTZ by the biexcitonic state of the QD.

Table 1. Time Constants for Hole Trapping (τ_{rise1}, τ_{decay1}), Decay of Trapped Holes (τ_{ave}), and Formation of $PTZ^{+\bullet}$ (τ_{hTi}) in PTC-Capped QD Samples, with Pump Energy = 0.2 μJ .[a]

	τ_{rise1}, ps λ_{probe} = 670 nm (A_{rise1})[b]	τ_{decay1}, ps λ_{probe} = 1400 nm (A_{decay1})[c]	τ_{ave}, ps λ_{probe} = 670 nm[d]	τ_{hT1}, ps $PTZ^{+\bullet}$ (A_1)[e]	τ_{hT2}, ps $PTZ^{+\bullet}$ (A_2)[e]	τ_{hT3}, ps $PTZ^{+\bullet}$ (A_3)[e]
	h^+ trapping	*h^+ trapping*	-	*direct h^+ transfer*	*trapped h^+ transfer*	*trapped h^+ transfer*
QD-PTC-C6	1.1±0.1 (-40%)	1.3±0.1 (75%)	1400±400	-	-	-
QD-PTC-*m*PTZ	0.8±0.1 (-30%)	0.8±0.1 (60%)	690±60	2.4±0.2 (47%)	35±5 (27%)	700±100 (26%)

[a]Time constants listed in this table are extracted from fits to kinetic traces of TA datasets at the indicated probe wavelengths, after pumping at 420 nm with 0.2 μJ pump energy. Analogous tables for other pump energies are in the SI. [b]A_{rise1} is the absolute % amplitude extracted from the fit to the kinetic trace at 670 nm attributable to hole trapping. This value is negative because it manifests a rise instead of a decay at this wavelength. [c]A_{decay1} is the % of the total amplitude of the decay of the signal at 1400 nm attributable to this component. [d]This time constant is the amplitude-averaged lifetime of decay of the signal at 670 nm. [e]This time constant is extracted from the fits to the deconvolved $PTZ^{+\bullet}$ kinetic traces; $\sum_{i=1}^{i=3} A_i = 1$.

Given this information about hole trapping rates and trapped hole lifetimes, we can assign the fastest component of $PTZ^{+\bullet}$ formation, τ_{hT1} = 2.4±0.2 ps at pump energy = 0.2 μJ, to the direct extraction of valence band holes to PTZ because (i) it is competitive with the fastest time constants for hole trapping (~1 ps); and (ii) despite a slight acceleration of hole trapping, the yield of hole trapping decreases upon introduction of PTZ, **Table 1**. This result suggests that fewer holes are trapping in CdS-PTC-*m*PTZ than in CdS-PTC-C6 because, we suspect, some of them are instead directly transferred to PTZ *via* direct extraction from the VB with time constant τ_{hT1}.

We can assign the second and third components of $PTZ^{+\bullet}$ formation, τ_{hT2} = 35±5 ps at 0.2 μJ and τ_{hT3} = 700±100 ps at 0.2 μJ, and faster at higher pump energies, see Table S3 of the SI, to transfer of a hole from a trap state at the QD/PTC interface to PTZ because (i) these processes are much slower than the rate of hole trapping, and (ii) a population of trapped holes present in CdS-PTC-C6 does not exist in CdS-PTC-*m*PTZ (**Figure 4B**). We suspect that population of initially trapped holes is being subsequently transferred to PTZ with time constants τ_{hT2} and τ_{hT3}.

Hole Transfer from QDs That Have Biexcitons. We have so far concluded that photoinduced hole transfer occurs directly from the VB of the QD to PTZ, and from trap states at the QD-PTC

interface. Here, we provide evidence for the extraction of holes specifically from biexcitonic states of QDs to PTZ. Our logic is that, if a QD is photo-oxidizing PTZ from a biexcitonic state, then the number of biexcitons that undergo Auger recombination should decrease upon introduction of PTZ. Furthermore, to prove that loss of Auger yield is attributable to photo-oxidation of PTZ by biexctions, there should be a direct correspondence between the decrease in the number (or percentage) of excitons that decay *via* Auger and the increase in the percentage of excitons that donate a hole to PTZ to form $PTZ^{+\bullet}$.

In this analysis, we again limit the number of excitons created per QD at any pump energy to two, bounded by the degeneracy of the band-edge excitonic state and our pump energy. At each pump energy, we calculate the percentage of QDs that have zero or one exciton (P_0, P_1) with the Poisson distribution $P_n = e^{-(\langle N \rangle)} \frac{(\langle N \rangle)^n}{n!}$, where n = 0, 1. Then, $P_2 = 1 - P_0 - P_1$, because we assume that all QDs that absorb two or more photons have biexcitons. The percentage of excitons within single or bi-excitonic states that are available to decay through Auger recombination ("Theoretical Auger %") is $\frac{P_2}{P_1+P_2}\frac{1}{2}$. The prefactor $\frac{1}{2}$ indicates that a maximum of one exciton within a biexciton can undergo Auger recombination before decaying *via* another pathway (we see no evidence that Auger recombination of trions occurs in a significant population of QDs, and that recombination pathway almost certainly has a time constant distinct from that we assign to biexciton Auger recombination). The percentage of excitons in the ensemble that actually do undergo Auger recombination ("Actual Auger %") is the normalized amplitude of the 20-ps Auger component of the total GSB decay in the TA spectrum of each sample. The Auger yield at each excitation density is defined as (Actual Auger %)/(Theoretical Auger %), and these values are listed in **Table 2**.

Table 2. Auger Yields in CdS-PTC-C6 and CdS-PTC-*m*PTZ Samples.

Pump Energy (μJ)	Theoretical Auger %[a]	Actual Auger % (CdS-PTC-C6)[b]	Actual Auger % (CdS-PTC-*m*PTZ)[b]	**Auger Yield (CdS-PTC-C6)[c]**	**Auger Yield (CdS-PTC-*m*PTZ)[c]**
0.2	0	0	0	**0**	**0**
0.6	17	8	7	**47**	**41**
1.0	31	17	13	**54**	**42**
1.6	38	26	19	**68**	**50**
2.0	44	28	19	**63**	**43**

[a] The detailed calculation of single and biexciton populations is included in Table S5 of the SI. [b]Extracted from the fits to the GSB kinetic traces. [c]Defined in the text.

For CdS-PTC-C6 samples, the Auger yield increases with increasing pump energy, until decreasing slightly at pump energy = 2.0 μJ. For CdS-PTC-*m*PTZ samples, the Auger yield is lower than that of CdS-PTC-C6 at pump energies. Since the excitation pump energies and sample concentrations are the same for samples with and without PTZ, we hypothesize that the differences in the Auger yields between CdS-PTC-C6 and CdS-PTC-*m*PTZ, listed as "Loss in Auger Yield" in **Table 3**, are due to extraction of holes from biexcitons of QDs to PTZ molecules.

Table 3. The % of the Biexciton Population in CdS QDs that (i) No Longer Decayed by Auger Recombination, and (ii) Decayed by Hole Transfer, upon Introduction of PTZ.

Pump Energy (μJ)	Loss in Auger Yield (%)[a]	X_2 (%)[b]
0.2	0	0
0.6	6	8
1.0	12	12
1.6	18	20
2.0	20	21

[a] Defined as "Auger Yield (CdS-PTC-C6)" - "Auger Yield (CdS-PTC-*m*PTZ)" from **Table 2**. [b]Defined as the percent yield of extraction of a hole from a biexciton within CdS-PTC-*m*PTZ, eq 1. X_2, by definition, is 0 for CdS-PTC-C6.

To test this hypothesis, we calculate the yield of hole extraction from biexcitons of QDs at different pump energies and compare it to the decrease in Auger yield at that pump energy. The yield of hole extraction from a QD that, upon photoexcitation, contains *n* excitons, X_n, is related to the concentration of $PTZ^{+\bullet}$ measured by TA ($[PTZ^{+\bullet}]$) through eq 1. X_1 is the yield of extraction of a hole from a QD

$$[PTZ^{+\bullet}] = \sum_{n=1}^{n=2} X_n P_n [QD] \qquad (1)$$

that forms a single exciton upon photoexcitation. X_2 is the yield of extraction of a hole from a QD that forms a biexciton upon photoexcitation. For the biexciton, X_2 is an average yield, specifically the weighted average of the yields of extracting one hole from the biexciton and of extracting two holes from the biexciton. Again, P_n is the probability of creating *n* excitons in a QD, and [QD] is the concentration of QDs, see the SI for details. We do not specify whether a hole extracted from a biexciton originates from the biexcitonic state or the single-exciton state that originates from a biexciton in this calculation.

We calculate [$PTZ^{+\bullet}$] from the TA signal of the $PTZ^{+\bullet}$ radical feature and an experimentally measured extinction coefficient (ε = 8000 $cm^{-1}M^{-1}$ at 520 nm, similar to the reported value for the un-functionalized PTZ[68], 9300 $cm^{-1}M^{-1}$). This analysis shows that X_1 = 13% – that, is, the yield of extracting one hole from a single exciton is 13%. We assume that X_1 is constant at pump energies since it is not related to the yield of Auger recombination. We then calculate X_2 for each pump energy and list the results in **Table 3**. For example, when pump energy = 0.6 μJ, X_2 = 8% – that is, at this pump energy, the average yield of hole transfer from a QD that was photoexcited to a biexcitonic state is 8%. If we assume, based simply on the low overall yield of hole extraction, that no biexciton transfers both holes to separate PTZs on the same QD, then we can conclude that 8% of QDs excited to a biexcitonic state transfer one hole to a PTZ. That yield is 21% for pump energy = 2 μJ.

The agreement between the two columns of data in **Table 3** indicates that we can account for all of the biexciton population that stop participating in Auger recombination upon introduction of PTZ with biexcitons that participate in hole transfer to PTZ. Recall that these two columns of data are derived from TA signals of two separate species: the loss in Auger yield from the normalized amplitude of the Auger component of the GSB of the QDs, and X_2 from the magnitude of the $PTZ^{+\bullet}$ signal at 520 nm. Their quantitative correspondence at all pump energies therefore strongly indicates that we are extracting holes from the biexcitonic states of QDs (rather than the single excitons to which biexcitons decay). In fact, this correspondence indicates that *all* of the holes extracted from QDs that initially contain two excitons come from the biexcitonic state. We suspect, but have not proven, that single excitons formed from biexcitonic precursors do not participate in hole transfer because Auger recombination leaves the high-energy exciton formed through impact ionization vulnerable to thermalization of hot holes to localized trap states that are not coupled electronically to PTZ.

CONCLUSIONS

In summary, when CdS QDs are capped with exciton delocalizing PTC ligands, photoinduced holes undergo ultrafast trapping in ~1 ps. When a hole acceptor PTZ is covalently attached to the *meta* position of the phenyl ring of the PTC moiety, holes can be extracted directly from the valence band of QDs by PTZ to form $PTZ^{+\bullet}$ in 2.4 ps, or trapped at the QD/PTC interface (in ~ 1 ps) and subsequently oxidize PTZ in tens-to-hundreds of ps. Comparison of the yield of Auger recombination (which occurs in ~20 ps) for QD samples with and without adsorbed PTZ,

combined with the pump-energy dependence of the yield of $PTZ^{+\bullet}$, reveals that PTZ is photo-oxidized by biexcitonic states of QDs, with yields of 8 – 21%.

This work shows that the PTC linker is a good strategy for the ultimate goal of extracting two holes from a biexciton to a single molecular acceptor, in order to photo-trigger oxidative two-electron chemistry. The PTC linker both (i) strongly electronically couples the organic hole acceptor to the QD core, resulting in fast direct hole transfer from the QD core to the molecule (even faster if the hole acceptor is connected in the *para*-position of the linker[39, 69-70]), and (ii) serves as an interfacial hole trap to quickly extract holes from transient excitonic states and then pass those holes onto the terminal acceptor. This work also demonstrates that hole extraction can out-compete Auger recombination, but that extracting both holes from a biexciton may require passivation strategies that eliminate trapping of hot holes to localized surface states.

SUPPORTING INFORMATION

Synthesis of PTC-*m*PTZ, NMR data, determination of the surface ligand coverage, description of the TA setup, and additional TA data and analyses. This information is available free of charge via the internet at http://pubs.acs.org.

ACKNOWLEDGEMENT

This project is primarily supported by the National Science Foundation under Award CHE-1664184 (QD synthesis, NMR experiments, and optical measurements), and by the Center for Light Energy Activated Redox Processes (LEAP), an Energy Frontier Research Center funded by the U.S. Department of Energy (DOE), Office of Science, Basic Energy Sciences (BES), under Award DE-SC0001059 (synthesis and chemical analysis). C.R.R. thanks the International Institute for Nanotechnology (IIN) at Northwestern University for a fellowship (synthesis). M.S.K. thanks the PPG Foundation for a graduate fellowship (calculations). The authors thank Prof. Ryan Young and Dr. Kedy Edme for helpful discussions.

REFERENCES

1. Huang, C.; Li, X.-B.; Tung, C.-H.; Wu, L.-Z., Photocatalysis with Quantum Dots and Visible Light for Effective Organic Synthesis. *Chem. Eur. J.* **2018,** *24*, 11530-11534.

2. McClelland, K. P.; Weiss, E. A., Selective Photocatalytic Oxidation of Benzyl Alcohol to Benzaldehyde or C–C Coupled Products by Visible-Light-Absorbing Quantum Dots. *ACS Appl. Energy Mater.* **2018**, *2*, 92-96.
3. Huang, Y.; Zhu, Y.; Egap, E., Semiconductor Quantum Dots as Photocatalysts for Controlled Light-Mediated Radical Polymerization. *ACS Macro Lett.* **2018,** *7*, 184-189.
4. Jensen, S. C.; Bettis Homan, S.; Weiss, E. A., Photocatalytic Conversion of Nitrobenzene to Aniline through Sequential Proton-Coupled One-Electron Transfers from a Cadmium Sulfide Quantum Dot. *J. Am. Chem. Soc.* **2016,** *138*, 1591-1600.
5. Lian, S.; Kodaimati, M. S.; Dolzhnikov, D. S.; Calzada, R.; Weiss, E. A., Powering a CO_2 Reduction Catalyst with Visible Light through Multiple Sub-Picosecond Electron Transfers from a Quantum Dot. *J. Am. Chem. Soc.* **2017,** *139*, 8931-8938.
6. Zhang, Z.; Edme, K.; Lian, S.; Weiss, E. A., Enhancing the Rate of Quantum-Dot-Photocatalyzed Carbon–Carbon Coupling by Tuning the Composition of the Dot's Ligand Shell. *J. Am. Chem. Soc.* **2017,** *139*, 4246-4249.
7. Caputo, J. A.; Frenette, L. C.; Zhao, N.; Sowers, K. L.; Krauss, T. D.; Weix, D. J., General and Efficient C–C Bond Forming Photoredox Catalysis with Semiconductor Quantum Dots. *J. Am. Chem. Soc.* **2017,** *139*, 4250-4253.
8. Simlandy, A. K.; Bhattacharyya, B.; Pandey, A.; Mukherjee, S., Picosecond Electron Transfer from Quantum Dots Enables a General and Efficient Aerobic Oxidation of Boronic Acids. *ACS Catal.* **2018,** *8*, 5206-5211.
9. Xi, Z.-W.; Yang, L.; Wang, D.-Y.; Pu, C.-D.; Shen, Y.-M.; Wu, C.-D.; Peng, X.-G., Visible-Light Photocatalytic Synthesis of Amines from Imines Via Transfer Hydrogenation Using Quantum Dots as Catalysts. *J. Org. Chem.* **2018,** *83*, 11886-11895.
10. Kodaimati, M. S.; Lian, S.; Schatz, G. C.; Weiss, E. A., Energy Transfer-Enhanced Photocatalytic Reduction of Protons within Quantum Dot Light-Harvesting–Catalyst Assemblies. *Proc. Natl. Acad. Sic. U.S.A.* **2018**, *115*, 8290-8295.
11. Lv, H.; Wang, C.; Li, G.; Burke, R.; Krauss, T. D.; Gao, Y.; Eisenberg, R., Semiconductor Quantum Dot-Sensitized Rainbow Photocathode for Effective Photoelectrochemical Hydrogen Generation. *Proc. Natl. Acad. Sic. U.S.A.* **2017,** *114*, 11297-11302.
12. Lian, S.; Kodaimati, M. S.; Weiss, E. A., Photocatalytically Active Superstructures of Quantum Dots and Iron Porphyrins for Reduction of CO_2 to CO in Water. *ACS Nano* **2018,** *12*, 568-575.
13. Kuehnel, M. F.; Orchard, K. L.; Dalle, K. E.; Reisner, E., Selective Photocatalytic CO_2 Reduction in Water through Anchoring of a Molecular Ni Catalyst on CdS Nanocrystals. *J. Am. Chem. Soc.* **2017,** *139*, 7217-7223.
14. Kuehnel, M. F.; Sahm, C. D.; Neri, G.; Lee, J. R.; Orchard, Katherine L.; Cowan, A. J.; Reisner, E., ZnSe Quantum Dots Modified with a Ni(Cyclam) Catalyst for Efficient Visible-Light Driven CO_2 Reduction in Water. *Chem. Sci.* **2018,** *9*, 2501-2509.
15. Wolff, C. M.; Frischmann, P. D.; Schulze, M.; Bohn, B. J.; Wein, R.; Livadas, P.; Carlson, M. T.; Jäckel, F.; Feldmann, J.; Würthner, F., et al., All-in-One Visible-Light-Driven Water Splitting by Combining Nanoparticulate and Molecular Co-Catalysts on CdS Nanorods. *Nat. Energy.* **2018,** *3*, 862-869.
16. Young, R. M.; Jensen, S. C.; Edme, K.; Wu, Y.; Krzyaniak, M. D.; Vermeulen, N. A.; Dale, E. J.; Stoddart, J. F.; Weiss, E. A.; Wasielewski, M. R., et al., Ultrafast Two-Electron

Transfer in a CdS Quantum Dot–Extended-Viologen Cyclophane Complex. *J. Am. Chem. Soc.* **2016,** *138*, 6163-6170.
17. Efros, A. L.; Rosen, M.; Kuno, M.; Nirmal, M.; Norris, D. J.; Bawendi, M., Band-Edge Exciton in Quantum Dots of Semiconductors with a Degenerate Valence Band: Dark and Bright Exciton States. *Phys. Rev. B* **1996,** *54*, 4843-4856.
18. Wise, F. W., Lead Salt Quantum Dots: The Limit of Strong Quantum Confinement. *Acc. Chem. Res.* **2000,** *33*, 773-780.
19. Kambhampati, P., Multiexcitons in Semiconductor Nanocrystals: A Platform for Optoelectronics at High Carrier Concentration. *J. Phys. Chem. Lett.* **2012,** *3*, 1182-1190.
20. Beard, M. C., Multiple Exciton Generation in Semiconductor Quantum Dots. *J. Phys. Chem. Lett.* **2011,** *2*, 1282-1288.
21. Ellingson, R. J.; Beard, M. C.; Johnson, J. C.; Yu, P.; Micic, O. I.; Nozik, A. J.; Shabaev, A.; Efros, A. L., Highly Efficient Multiple Exciton Generation in Colloidal PbSe and PbS Quantum Dots. *Nano Lett.* **2005,** *5*, 865-871.
22. Ji, M.; Park, S.; Connor, S. T.; Mokari, T.; Cui, Y.; Gaffney, K. J., Efficient Multiple Exciton Generation Observed in Colloidal PbSe Quantum Dots with Temporally and Spectrally Resolved Intraband Excitation. *Nano Lett.* **2009,** *9*, 1217-1222.
23. Klimov, V. I.; Mikhailovsky, A. A.; McBranch, D. W.; Leatherdale, C. A.; Bawendi, M. G., Quantization of Multiparticle Auger Rates in Semiconductor Quantum Dots. *Science* **2000,** *287*, 1011-1013.
24. Stewart, J. T.; Padilha, L. A.; Qazilbash, M. M.; Pietryga, J. M.; Midgett, A. G.; Luther, J. M.; Beard, M. C.; Nozik, A. J.; Klimov, V. I., Comparison of Carrier Multiplication Yields in PbS and PbSe Nanocrystals: The Role of Competing Energy-Loss Processes. *Nano Lett.* **2012,** *12*, 622-628.
25. Oron, D.; Kazes, M.; Banin, U., Multiexcitons in Type-II Colloidal Semiconductor Quantum Dots. *Phys. Rev. B* **2007,** *75*, 035330.
26. Klimov, V. I., Spectral and Dynamical Properties of Multiexcitons in Semiconductor Nanocrystals. *Annu. Rev. Phys. Chem.* **2007,** *58*, 635-673.
27. Zhu, H.; Lian, T., Wavefunction Engineering in Quantum Confined Semiconductor Nanoheterostructures for Efficient Charge Separation and Solar Energy Conversion. *Energy Environ. Sci* **2012,** *5*, 9406-9418.
28. Zhu, H.; Song, N.; Rodríguez-Córdoba, W.; Lian, T., Wave Function Engineering for Efficient Extraction of up to Nineteen Electrons from One CdSe/CdS Quasi-Type II Quantum Dot. *J. Am. Chem. Soc.* **2012,** *134*, 4250-4257.
29. Kaledin, A. L.; Kong, D.; Wu, K.; Lian, T.; Musaev, D. G., Quantum Confinement Theory of Auger-Assisted Biexciton Recombination Dynamics in Type-I and Quasi Type-II Quantum Dots. *J. Phys. Chem. C* **2018,** *122*, 18742-18750.
30. Wu, K.; Liang, G.; Kong, D.; Chen, J.; Chen, Z.; Shan, X.; McBride, J. R.; Lian, T., Quasi-Type II $CuInS_2$/CdS Core/Shell Quantum Dots. *Chem. Sci.* **2016,** *7*, 1238-1244.
31. Zhu, H.; Yang, Y.; Lian, T., Multiexciton Annihilation and Dissociation in Quantum Confined Semiconductor Nanocrystals. *Acc. Chem. Res.* **2013,** *46*, 1270-1279.
32. Morris-Cohen, A. J.; Frederick, M. T.; Cass, L. C.; Weiss, E. A., Simultaneous Determination of the Adsorption Constant and the Photoinduced Electron Transfer Rate for a Cds Quantum Dot–Viologen Complex. *J. Am. Chem. Soc.* **2011,** *133*, 10146-10154.

33. Knowles, K. E.; Malicki, M.; Weiss, E. A., Dual-Time Scale Photoinduced Electron Transfer from PbS Quantum Dots to a Molecular Acceptor. *J. Am. Chem. Soc.* **2012,** *134*, 12470-12473.
34. Wang, J.; Ding, T.; Wu, K., Electron Transfer into Electron-Accumulated Nanocrystals: Mimicking Intermediate Events in Multielectron Photocatalysis II. *J. Am. Chem. Soc.* **2018,** *140*, 10117-10120.
35. Huang, J.; Huang, Z.; Yang, Y.; Zhu, H.; Lian, T., Multiple Exciton Dissociation in CdSe Quantum Dots by Ultrafast Electron Transfer to Adsorbed Methylene Blue. *J. Am. Chem. Soc.* **2010,** *132*, 4858-4864.
36. Kamat, P. V.; Christians, J. A.; Radich, J. G., Quantum Dot Solar Cells: Hole Transfer as a Limiting Factor in Boosting the Photoconversion Efficiency. *Langmuir* **2014,** *30*, 5716-5725.
37. Ding, T. X.; Olshansky, J. H.; Leone, S. R.; Alivisatos, A. P., Efficiency of Hole Transfer from Photoexcited Quantum Dots to Covalently Linked Molecular Species. *J. Am. Chem. Soc.* **2015,** *137*, 2021-2029.
38. Jin, X.; Chang, C.; Zhao, W.; Huang, S.; Gu, X.; Zhang, Q.; Li, F.; Zhang, Y.; Li, Q., Balancing the Electron and Hole Transfer for Efficient Quantum Dot Light-Emitting Diodes by Employing a Versatile Organic Electron-Blocking Layer. *ACS Appl. Mater. Interfaces* **2018,** *10*, 15803-15811.
39. Lian, S.; Weinberg, D. J.; Harris, R. D.; Kodaimati, M. S.; Weiss, E. A., Subpicosecond Photoinduced Hole Transfer from a CdS Quantum Dot to a Molecular Acceptor Bound through an Exciton-Delocalizing Ligand. *ACS Nano* **2016,** *10*, 6372-6382.
40. Sambur, J. B.; Novet, T.; Parkinson, B. A., Multiple Exciton Collection in a Sensitized Photovoltaic System. *Science* **2010,** *330*, 63.
41. Frederick, M. T.; Weiss, E. A., Relaxation of Exciton Confinement in CdSe Quantum Dots by Modification with a Conjugated Dithiocarbamate Ligand. *ACS Nano* **2010,** *4*, 3195-3200.
42. Jin, S.; Harris, R. D.; Lau, B.; Aruda, K. O.; Amin, V. A.; Weiss, E. A., Enhanced Rate of Radiative Decay in CdSe Quantum Dots Upon Adsorption of an Exciton-Delocalizing Ligand. *Nano Lett.* **2014,** *14*, 5323-5328.
43. Frederick, M. T.; Amin, V. A.; Cass, L. C.; Weiss, E. A., A Molecule to Detect and Perturb the Confinement of Charge Carriers in Quantum Dots. *Nano Lett.* **2011,** *11*, 5455-5460.
44. Frederick, M. T.; Amin, V. A.; Swenson, N. K.; Ho, A. Y.; Weiss, E. A., Control of Exciton Confinement in Quantum Dot–Organic Complexes through Energetic Alignment of Interfacial Orbitals. *Nano Lett.* **2013,** *13*, 287-292.
45. Azzaro, M. S.; Babin, M. C.; Stauffer, S. K.; Henkelman, G.; Roberts, S. T., Can Exciton-Delocalizing Ligands Facilitate Hot Hole Transfer from Semiconductor Nanocrystals? *J. Phys. Chem. C* **2016,** *120*, 28224-28234.
46. La Croix, A. D.; O'Hara, A.; Reid, K. R.; Orfield, N. J.; Pantelides, S. T.; Rosenthal, S. J.; Macdonald, J. E., Design of a Hole Trapping Ligand. *Nano Lett.* **2017,** *17*, 909-914.
47. Lee, J. R.; Li, W.; Cowan, A. J.; Jäckel, F., Hydrophilic, Hole-Delocalizing Ligand Shell to Promote Charge Transfer from Colloidal CdSe Quantum Dots in Water. *J. Phys. Chem. C* **2017,** *121*, 15160-15168.
48. Azzaro, M. S.; Dodin, A.; Zhang, D. Y.; Willard, A. P.; Roberts, S. T., Exciton-Delocalizing Ligands Can Speed up Energy Migration in Nanocrystal Solids. *Nano Lett.* **2018,** *18*, 3259-3270.

49. Teunis, M. B.; Nagaraju, M.; Dutta, P.; Pu, J.; Muhoberac, B. B.; Sardar, R.; Agarwal, M., Elucidating the Role of Surface Passivating Ligand Structural Parameters in Hole Wave Function Delocalization in Semiconductor Cluster Molecules. *Nanoscale* **2017,** *9*, 14127-14138.
50. Xie, Y.; Teunis, M. B.; Pandit, B.; Sardar, R.; Liu, J., Molecule-Like CdSe Nanoclusters Passivated with Strongly Interacting Ligands: Energy Level Alignment and Photoinduced Ultrafast Charge Transfer Processes. *J. Phys. Chem. C* **2015,** *119*, 2813-2821.
51. McArthur, E. A.; Morris-Cohen, A. J.; Knowles, K. E.; Weiss, E. A., Charge Carrier Resolved Relaxation of the First Excitonic State in CdSe Quantum Dots Probed with near-Infrared Transient Absorption Spectroscopy. *J. Phys. Chem. B* **2010,** *114*, 14514-14520.
52. Harris, R. D.; Amin, V. A.; Lau, B.; Weiss, E. A., Role of Interligand Coupling in Determining the Interfacial Electronic Structure of Colloidal CdS Quantum Dots. *ACS Nano* **2016**, *10*, 1395-1403.
53. Yu, W. W.; Qu, L.; Guo, W.; Peng, X., Experimental Determination of the Extinction Coefficient of CdTe, CdSe, and CdS Nanocrystals. *Chem. Mater.* **2003,** *15*, 2854-2860.
54. Horodyská, P.; Němec, P.; Sprinzl, D.; Malý, P.; Gladilin, V. N.; Devreese, J. T., Exciton Spin Dynamics in Spherical CdS Quantum Dots. *Phys. Rev. B* **2010,** *81*, 045301.
55. Fonoberov, V. A.; Pokatilov, E. P.; Balandin, A. A., Exciton States and Optical Transitions in Colloidal CdS Quantum Dots: Shape and Dielectric Mismatch Effects. *Phys. Rev. B* **2002,** *66*, 085310.
56. Shulenberger, K. E.; Bischof, T. S.; Caram, J. R.; Utzat, H.; Coropceanu, I.; Nienhaus, L.; Bawendi, M. G., Multiexciton Lifetimes Reveal Triexciton Emission Pathway in CdSe Nanocrystals. *Nano Lett.* **2018,** *18*, 5153-5158.
57. Cooney, R. R.; Sewall, S. L.; Sagar, D. M.; Kambhampati, P., Gain Control in Semiconductor Quantum Dots Via State-Resolved Optical Pumping. *Phys. Rev. Lett.* **2009,** *102*, 127404.
58. Krause, M. M.; Kambhampati, P., Linking Surface Chemistry to Optical Properties of Semiconductor Nanocrystals. *Phys. Chem. Chem. Phys.* **2015,** *17*, 18882-18894.
59. Walsh, B. R.; Saari, J. I.; Krause, M. M.; Nick, R.; Coe-Sullivan, S.; Kambhampati, P., Surface and Interface Effects on Non-Radiative Exciton Recombination and Relaxation Dynamics in CdSe/Cd,Zn,S Nanocrystals. *Chem. Phys.* **2016,** *471*, 11-17.
60. Saari, J. I.; Dias, E. A.; Reifsnyder, D.; Krause, M. M.; Walsh, B. R.; Murray, C. B.; Kambhampati, P., Ultrafast Electron Trapping at the Surface of Semiconductor Nanocrystals: Excitonic and Biexcitonic Processes. *J. Phys. Chem. B* **2013,** *117*, 4412-4421.
61. Huang, J.; Huang, Z.; Jin, S.; Lian, T., Exciton Dissociation in CdSe Quantum Dots by Hole Transfer to Phenothiazine. *J. Phys. Chem. C* **2008,** *112*, 19734-19738.
62. Schnitzenbaumer, K. J.; Labrador, T.; Dukovic, G., Impact of Chalcogenide Ligands on Excited State Dynamics in CdSe Quantum Dots. *J. Phys. Chem. C* **2015,** *119*, 13314-13324.
63. Margulies, E. A.; Wu, Y.-L.; Gawel, P.; Miller, S. A.; Shoer, L. E.; Schaller, R. D.; Diederich, F.; Wasielewski, M. R., Sub-Picosecond Singlet Exciton Fission in Cyano-Substituted Diaryltetracenes. *Angew. Chem. Int. Ed.* **2015,** *54*, 8679-8683.
64. Wu, K.; Du, Y.; Tang, H.; Chen, Z.; Lian, T., Efficient Extraction of Trapped Holes from Colloidal CdS Nanorods. *J. Am. Chem. Soc.* **2015,** *137*, 10224-10230.
65. Knowles, K. E.; McArthur, E. A.; Weiss, E. A., A Multi-Timescale Map of Radiative and Nonradiative Decay Pathways for Excitons in CdSe Quantum Dots. *ACS Nano* **2011,** *5*, 2026-2035.

66. Jin, S.; Tagliazucchi, M.; Son, H.-J.; Harris, R. D.; Aruda, K. O.; Weinberg, D. J.; Nepomnyashchii, A. B.; Farha, O. K.; Hupp, J. T.; Weiss, E. A., Enhancement of the Yield of Photoinduced Charge Separation in Zinc Porphyrin–Quantum Dot Complexes by a Bis(Dithiocarbamate) Linkage. *J. Phys. Chem. C* **2015,** *119*, 5195-5202.
67. Aruda, K. O.; Amin, V. A.; Thompson, C. M.; Lau, B.; Nepomnyashchii, A. B.; Weiss, E. A., Description of the Adsorption and Exciton Delocalizing Properties of P-Substituted Thiophenols on CdSe Quantum Dots. *Langmuir* **2016,** *32*, 3354-3364.
68. Alkaitis, S. A.; Beck, G.; Graetzel, M., Laser Photoionization of Phenothiazine in Alcoholic and Aqueous Micellar Solution. Electron Transfer from Triplet States to Metal Ion Acceptors. *J. Am. Chem. Soc.* **1975,** *97*, 5723-5729.
69. Ahn, T. S.; Thompson, A. L.; Bharathi, P.; Müller, A.; Bardeen, C. J., Light-Harvesting in Carbonyl-Terminated Phenylacetylene Dendrimers: The Role of Delocalized Excited States and the Scaling of Light-Harvesting Efficiency with Dendrimer Size. *J. Phys. Chem. B* **2006,** *110*, 19810-19819.
70. Thompson, A. L.; Ahn, T.-S.; Thomas, K. R. J.; Thayumanavan, S.; Martínez, T. J.; Bardeen, C. J., Using Meta Conjugation to Enhance Charge Separation Versus Charge Recombination in Phenylacetylene Donor−Bridge−Acceptor Complexes. *J. Am. Chem. Soc.* **2005,** *127*, 16348-16349.

TOC Graphic